View metadata, citation and similar papers at core.ac.uk

brought to you by CORE

provided by Elsevier - Publisher Connector

Cell, Vol. 101, 801–811, June 23, 2000, Copyright ©2000 by Cell Press

Crystal Structure of the λ Repressor C-Terminal Domain Provides a Model for Cooperative Operator Binding

Charles E. Bell,* Paolo Frescura,*
Ann Hochschild,† and Mitchell Lewis*‡
*The Johnson Foundation and
Department of Biochemistry and Biophysics
University of Pennsylvania School of Medicine
Philadelphia, Pennsylvania 19104
†Department of Microbiology and Molecular Genetics
Harvard Medical School
Boston, Massachusetts 02115

Summary

Interactions between transcription factors bound to separate operator sites commonly play an important role in gene regulation by mediating cooperative binding to the DNA. However, few detailed structural models for understanding the molecular basis of such cooperativity are available. The *c*I repressor of bacteriophage λ is a classic example of a protein that binds to its operator sites cooperatively. The C-terminal domain of the repressor mediates dimerization as well as a dimer–dimer interaction that results in the cooperative binding of two repressor dimers to adjacent operator sites. Here, we present the x-ray crystal structure of the λ repressor C-terminal domain determined by multiwavelength anomalous diffraction. Remarkably, the interactions that mediate cooperativity are captured in the crystal, where two dimers associate about a 2-fold axis of symmetry. Based on the structure and previous genetic and biochemical data, we present a model for the cooperative binding of two λ repressor dimers at adjacent operator sites.

Introduction

The ability of bacteriophage λ to replicate either lysogenically or lytically is tightly controlled by a "genetic switch" (Ptashne, 1992). During lysogenic growth, the viral genes are turned off, and the phage replicates quiescently along with the host. Upon induction of the lytic pathway, the genes required for phage assembly are turned on and the host is ultimately lysed. The switch not only insures that the stability of lysogeny can be maintained but also that lytic growth can be efficiently induced if the survival of the host cell is threatened. The molecular mechanism of the genetic switch was dissected in large part through the work of Ptashne and colleagues.

A key component of the switch is the repressor, the product of the *c*I gene. The λ repressor controls the expression of the viral genes by binding to six operator sites located within the left and right operator regions (O_R and O_L) of the λ chromosome (Maniatis and Ptashne, 1973; Maniatis et al., 1975). O_R and O_L, which are ~2500 bp apart, each contain three discrete 17 bp operator sites separated by 3–7 bp linkers. The repressor binds to each of these sites as a dimer. Because the operator sites are not identical in sequence, the intrinsic affinity of the repressor for each of the individual sites varies, with that for $O_R1 > O_R2 \approx O_R3$.

The λ repressor binds cooperatively to adjacent operator sites (Johnson et al., 1979). Cooperativity arises from a favorable interaction between two repressor dimers, as they are brought together on the DNA. Within O_R, the binding of one dimer to the high-affinity site O_R1 facilitates the binding of a second dimer to the lower-affinity site O_R2. Cooperativity increases the apparent affinity of the repressor for O_R2 such that both O_R1 and O_R2 are occupied at the concentrations of repressor in a lysogen. The cooperatively bound pair of repressor dimers prevents *E. coli* RNA polymerase from binding to the lytic promoter P_R and thereby prevents the expression of genes required for lytic growth (Meyer et al., 1980). In addition, the repressor dimer bound to O_R2 facilitates the productive interaction of RNA polymerase with the lysogenic promoter for repressor maintenance (P_{RM}) and thereby activates transcription of the *c*I gene (Meyer and Ptashne, 1980; Guarente et al., 1982; Hochschild et al., 1983; Bushman et al., 1989; Kuldell and Hochschild, 1994; Li et al., 1994).

Cooperativity is essential for maintaining lysogeny. Phage bearing a mutant repressor defective in cooperative binding form clear plaques due to their inability to form stable lysogens (Benson et al., 1994). Moreover, cooperativity amplifies the sensitivity of the switch that controls prophage induction, since large changes in fractional occupancy of the operator sites occur over a relatively narrow range of repressor concentrations (Ackers et al., 1982). Although repressor dimers bind cooperatively to adjacent operator sites on the natural λ chromosome, repressor dimers can also bind cooperatively to operators separated by five or six turns of the DNA duplex, in which cases the intervening DNA is looped (Griffith et al., 1986; Hochschild and Ptashne, 1986).

The λ repressor consists of two domains tethered by an ~40-residue linker (Pabo et al., 1979). The N-terminal domain (NTD), residues 1–92, mediates binding of the repressor to the operator as well as its interaction with RNA polymerase at P_{RM}. The C-terminal domain (CTD), residues 132–236, mediates dimerization as well as the interactions responsible for the cooperative binding of two repressor dimers to pairs of operator sites. Although the isolated NTD forms a weak dimer in solution, the residues primarily responsible for dimerization are located within the CTD. At physiological concentrations (10^{-7} M) the intact repressor is predominantly dimeric ($K_d = 10^{-8}$ M), while at 100-fold higher concentrations the repressor forms tetramers and octamers (Sauer, 1979; Senear et al., 1993).

In addition to mediating dimerization and cooperativity, the λ repressor CTD catalyzes a self-cleavage reaction (Little, 1984). When a λ lysogen is exposed to an environmental stress that damages the host DNA, the virus alters its mode of replication by switching on the

‡To whom correspondence should be addressed (e-mail: lewis@mail.med.upenn.edu).

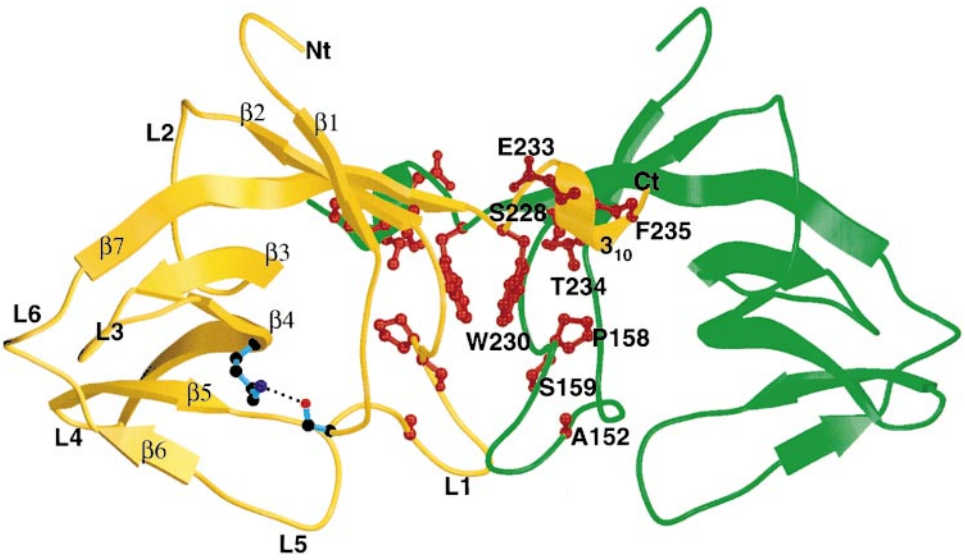

Figure 1. Structure of the λ Repressor C-Terminal Domain Dimer

The dimer in the asymmetric unit of the crystal is shown in ribbon representation. The view is perpendicular to the 2-fold axis of symmetry (noncrystallographic). The monomer on the left (gold) is shown with β strands labeled β1-β7, coil and turn regions L1-L6, and the 3_{10}-helix 3_{10}. Lys-192 and Ser-149, shown in blue ball-and-stick, form the active site for RecA-mediated cleavage. Residues shown in brown ball-and-stick (and labeled for the green subunit) are affected by mutations that inhibit dimerization. Notice that these residues map to the dimer interface. Also notice that the C-terminal 3_{10}-helices are "swapped."

lytic program of development. This event depends upon the deactivation of the repressor, which is accomplished by a proteolytic cleavage that separates the NTD from the CTD. Lacking the dimerization and cooperativity functions of the CTD, the isolated NTD no longer binds to the operator sites with sufficient affinity to maintain lysogeny. Though the cleavage depends on the presence of an activated form of the host's RecA protein, the active site for the reaction is formed by residues of the CTD of the repressor.

An extensive body of genetic and biochemical data that pertains to all aspects of repressor function has accumulated over the last three decades. However, detailed structural information is available only for the isolated NTD (Pabo and Lewis, 1982; Jordan and Pabo, 1988; Beamer and Pabo, 1992). To understand the structural basis of dimerization, cooperativity, and RecA-mediated cleavage, we have determined the x-ray crystal structure of the isolated CTD of the repressor. The structure, in concert with the previous studies, provides a model for how two repressor dimers interact cooperatively at pairs of operator sites on the DNA. In addition, the structure suggests a plausible mechanism for how the repressor forms an octamer.

Results

A gene fragment encoding residues 132–236 of the λ repressor, corresponding to the C-terminal fragment generated by papain cleavage (Pabo et al., 1979), was expressed in *E. coli*, and the resulting protein was purified and crystallized. The x-ray crystal structure was determined by multiwavelength anomalous diffraction (MAD) using data collected on a mercury derivative and refined to 1.9 Å resolution. There are two subunits of the CTD in the asymmetric unit of the crystal.

Structural Overview

The CTD forms a compact globular domain that consists of a highly twisted seven-stranded antiparallel β sheet followed by a single turn of 3_{10}-helix (Figure 1). Two long loops (loop 1 and loop 5) extend to one side of the monomer. In the asymmetric unit of the crystal, two subunits of the CTD form a dimer. Residues of loop 1, β strand 7, and the C-terminal 3_{10}-helix (residues 232–236) interact to stabilize the dimer, burying 911 $Å^2$ of solvent-accessible surface area per monomer. More specifically, residues of β strand 7 (Ser-228 and Trp-230) form antiparallel β sheet hydrogen bonds across the dimer interface. Specificity of this association is maintained by mainchain to sidechain hydrogen bonds between Trp-230 Ne1 and Ser-159′ O and between Phe-235 O and Lys-224′ Nζ. The C-terminal 3_{10}-helix also contributes significantly to the dimer formation, where the phenyl ring of Phe-235 of one subunit is bound to a hydrophobic pocket formed by several residues of the other subunit, including Val-225′, Phe-160′, and Phe-179′.

Several genetic screens have identified amino acid substitutions that affect the monomer-dimer equilibrium of the repressor (Cohen et al., 1981; Gimble and Sauer, 1985, 1989; Beckett et al., 1993; Burz et al., 1994; Whipple et al., 1994; J. Hu and R. T. Sauer, unpublished data). These amino acid substitutions, A152T, P158T, S159N, S228N, W230L, W230C, E233K, T234K, and F235I, involve residues at the dimer interface seen in the crystal (Figure 1), strongly suggesting that this dimer is physiologically relevant. The specific interactions seen in the crystal structure also implicate a number of residues in

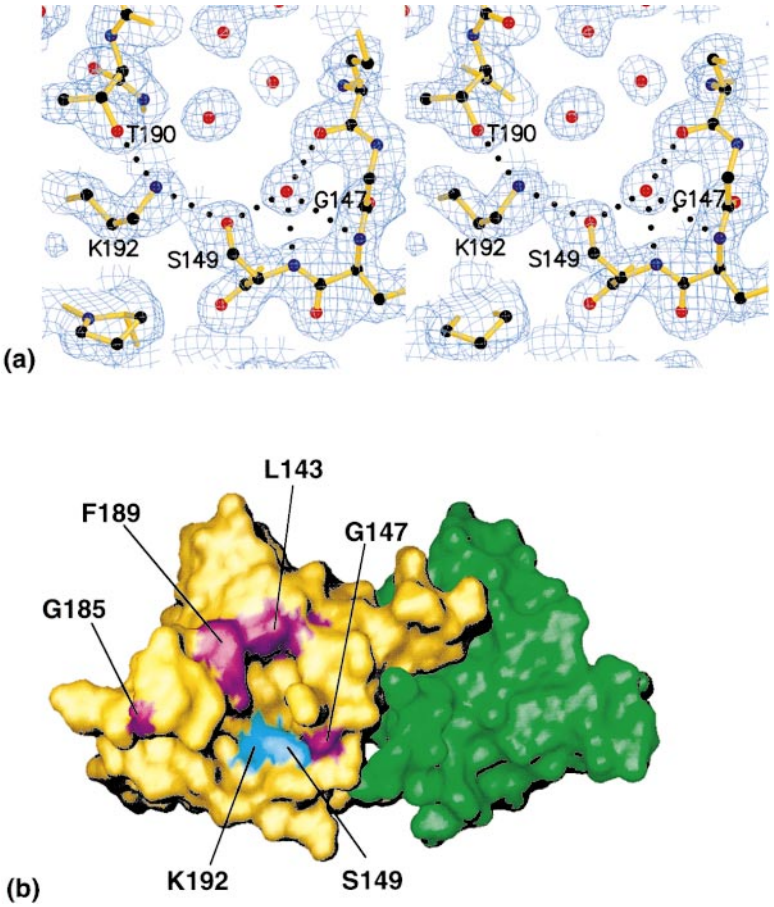

Figure 2. Residues of the λ Repressor C-Terminal Domain Involved in RecA-Mediated Cleavage

(A) Close-up view of the active site for RecA-mediated cleavage. The orientation is approximately the same as in Figure 1. The final 1.9 Å electron density map ($2F_o$-F_c) is superimposed on the structure and contoured at 1σ. Water molecules are shown as red spheres and hydrogen bonds as dotted lines. By deprotonation, Lys-192 is thought to activate Ser-149 for nucleophilic attack on the carbonyl carbon atom of the Ala-111-Gly-112 peptide bond (not present).

(B) A surface representation of the CTD dimer shows residues implicated in the RecA-mediated cleavage. The orientation is the same as in Figure 1. The active-site residues Ser-149 and Lys-192 are shown in cyan. Residues that are affected by *ind*⁻ mutations (defective in the RecA-mediated cleavage) are shown in purple. Notice that Phe-189 and Leu-143 form an exposed hydrophobic patch that could be a RecA binding site.

the monomer–monomer interaction that were not identified in the genetic screens. However, as these screens uncovered dimerization mutations indirectly, due to their effects on the RecA-mediated cleavage or on cooperativity, it is likely that only a subset of the possible dimerization mutants was isolated.

The overall fold of the CTD is similar to that of the *E. coli* UmuD′ protein (Peat et al., 1996a), as expected based on sequence similarity. The structures of the two monomers superimpose to an rms deviation of 0.98 Å for 81 pairs of Cα atoms. Moreover, the CTD dimer is similar to the UmuD′ dimer observed in solution by NMR and in the crystal structure where two UmuD′ monomers pack about a 2-fold axis of symmetry (Peat et al., 1996a; Ferentz et al., 1997). There are, however, significant differences between the two structures. The CTD has the insertion of residues 153–158 in loop 1 and a short 3_{10}-helix at the C terminus, each of which participates in dimer formation. The UmuD′ x-ray structure has an additional 12 residues at the N terminus, which associate in the crystal and were proposed to be involved in the formation of a UmuD′ filament (Peat et al., 1996b). The equivalent residues of the λ repressor are part of the linker region preceding the CTD and are not part of the crystallized protein fragment.

RecA-Mediated Cleavage

The switch from lysogenic to lytic development of phage λ is achieved by RecA-mediated cleavage of the Ala-111-Gly-112 peptide bond, resulting in the separation of the NTD from the CTD (Sauer et al., 1982). Several related lambdoid phage repressors, as well as the *E. coli* proteins UmuD and LexA, catalyze a similar self-cleavage reaction. A pair of strictly conserved residues, Ser-149 and Lys-192 in the λ repressor, is thought to participate in the reaction (Slilaty and Little, 1987). Although in vivo the cleavage is dependant on an activated form of the RecA protein, in vitro an autocleavage reaction occurs in the absence of RecA under mildly basic (pH ~10) conditions. These observations have led to a proposed mechanism in which the conserved lysine residue, in an unprotonated form, removes a proton from the serine residue, thereby activating it to perform a nucleophilic attack on the carbonyl carbon atom of the Ala-111-Gly-112 peptide bond (Slilaty and Little, 1987).

Consistent with such a mechanism, the structure shows that the Ser-149 Oγ atom is hydrogen bonded (3.1 Å) to the Lys-192 Nζ atom (Figure 2A). The two residues are located within a shallow groove on the surface of the CTD (Figure 2B). The structure also suggests a potential role for Thr-190, which is closely hydrogen bonded (2.7 Å) through its Oγ1 atom to the Lys-192 Nζ atom (Figure 2A). Conceivably, the interaction of Thr-190 could kinetically facilitate the deprotonation of Lys-192, which could in turn deprotonate Ser-149. Such a role for Thr-190 would be analogous to that of the aspartate residue in the Asp-His-Ser catalytic triad of some serine proteases (Dodson and Wlodawer, 1998). Alternatively, Thr-190 could help to orient precisely the Lys-192 sidechain to activate Ser-149 for nucleophilic attack.

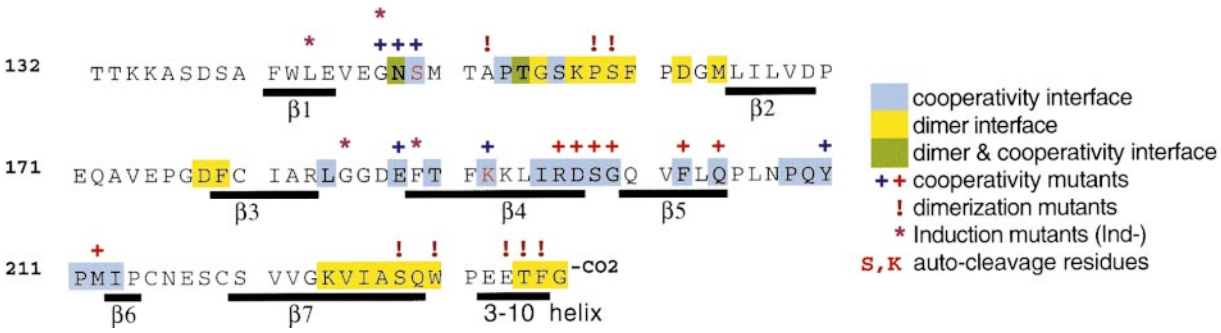

Figure 3. Mutations that Affect Dimerization and Cooperativity Coincide with Residues at the Dimer Interface and Dimer–Dimer Interface, Respectively

The sequence of the λ repressor CTD is shown (Thr-132-Gly-236) with a space inserted every ten residues. Residues at the dimer interface of the CTD (within 4 Å contact in the structure) are shaded in yellow. Similarly, residues at the cooperativity interface (dimer–dimer interface shown in Figure 4) are shaded in light blue, and residues at both interfaces are shaded in green. Residues affected by mutations that disrupt dimerization, cooperativity, or RecA-mediated cleavage are indicated above the sequence. For the cooperativity mutations, a red or blue "+" is assigned according to the patches of residues colored in Figure 4. Secondary structures of the CTD are indicated below the sequence. The invariant active site residues (Ser-149 and Lys-192) are highlighted in red letters. Notice that the residues identified by genetic data to be important for dimerization or cooperativity are in close agreement with the subunit-interfaces observed in the crystal.

Although mutagenesis studies probing the role of Thr-190 have not been reported, Thr-190 is conserved among enzymes that undergo RecA-mediated cleavage, except in the related lambdoid phage HKO22 *c*I repressor where His is found at the equivalent position. In LexA, the corresponding residue, Thr-154, gives a weak *ind*⁻ phenotype (see paragraph below for definition) when substituted with Ile (Lin and Little, 1989).

The mechanism by which RecA facilitates the cleavage reaction is not well understood. Several mutations of the *c*I gene prevent RecA-mediated cleavage of the λ repressor and thereby render the lysogen noninducible upon irradiation of the cells by UV (Gimble and Sauer, 1985). Such mutations, designated *ind*⁻, generally affect residues located in the vicinity of the cleavage site within the linker region. However, *ind*⁻ mutations have been isolated that affect four amino acid positions within the CTD. Based on in vitro analysis, three of the corresponding mutants, bearing the substitutions G185E, G185R, and F189L, are fully active in the autocleavage reaction at pH ~10 in the absence of RecA, despite being deficient in the RecA-mediated reaction (Gimble and Sauer, 1986). These *ind*⁻ amino acid substitutions appear to prevent the cleavage reaction by disrupting the interaction of the CTD with RecA. A fourth mutant, bearing the G147D substitution, shows zero levels of autocleavage, suggesting that this substitution directly disrupts either substrate binding or the active-site geometry. A fifth mutant, bearing the L143F substitution, shows intermediate levels of autocleavage (Gimble and Sauer, 1986).

The structure of the CTD shows that the four amino acid residues affected by *ind*- mutations are located on the surface of the protein in the vicinity of the active-site residues Ser-149 and Lys-192 (Figure 2B). Gly-147, which is strictly conserved among proteins that carry out the RecA-mediated cleavage, is located within 4 Å of Ser-149. In fact, a well-ordered water molecule, also seen in the UmuD′ structure, is bound by the Ser-149 Oγ atom, the backbone carbonyl of Glu-146, and the backbone amides of Asn-148 and Ser-149 (Figure 2A). This suggests that Gly-147 is crucial in forming the proper active-site geometry or perhaps in binding the Ala-111-Gly-112 peptide bond. The other three residues affected by *ind*⁻ mutations, Leu-143, Gly-185, and Phe-189, are located further from the active site but still within ~10 Å. The location of these residues relative to the active site suggests they could form a RecA binding site on the surface of the repressor. Particularly intriguing is the observation that Leu-143 and Phe-189 are part of an exposed apolar patch, surrounding the active site on the surface of the dimer (Figure 2B), as many protein–protein interactions are mediated by apolar residues (Jones and Thornton, 1996). Several other residues, including Phe-141, Val-222, Pro-170, Pro-211, Ile-213, and Leu-184, contribute exposed, apolar surface area in the vicinity of the active-site cleft.

The biochemical data suggest that only the repressor monomer can undergo RecA-mediated cleavage. Mutations that inhibit dimerization of the repressor increase its susceptibility to RecA-mediated cleavage. In addition, a repressor dimer stabilized by the introduction of an intersubunit disulfide bond is resistant to cleavage (Gimble and Sauer, 1989). One possible explanation for these observations is that the RecA binding site on the repressor overlaps with the dimerization interface, and thus dimerization prevents interaction with RecA. However, the structure shows that the residues affected by *ind*⁻ mutations do not coincide with the dimer interface (Figure 2B). A second possible explanation is that a conformational change in the repressor that is required for RecA-mediated cleavage is prevented by dimerization of the repressor.

Structural Basis of Cooperativity

Genetic studies have identified mutations that disrupt the cooperative binding of two λ repressor dimers to pairs of operator sites, while having no effect on the binding of a dimer to a single operator site (Beckett et al., 1993; Benson et al., 1994; Burz and Ackers, 1994; Whipple et al., 1994, 1998). Such mutations affect residues located within the CTD, at 13 different amino acid positions, as shown above the sequence in Figure 3.

These amino acids are predicted to lie at or near the interface formed when two repressor dimers are bound cooperatively. Based on second site suppressor mutation analysis, two pairs of amino acids, Lys-192-Asp-197 and Asn-148-Gln-204, are predicted to be juxtaposed at the dimer–dimer interface (Whipple et al., 1998).

The structure shows that the residues affected by cooperativity mutations cluster into discrete patches on the surface of the CTD dimer (Figure 4A). There are four such patches, with two on one monomer related by the 2-fold symmetry to two on the other monomer. Asp-197 and Gln-204 comprise part of the patch colored red in Figure 4A, while Lys-192 and Asn-148 comprise part of the patch colored blue. Thus, mapping the genetic data onto the structure of the CTD dimer implicates particular surface patches as probable sites of interaction between two repressor dimers. Moreover, the second site suppressor data suggest that the red patch (containing Asp-197 and Gln-204) interacts with the blue patch (containing Lys-192 and Asn-148).

In the crystal, two CTD dimers associate about a 2-fold axis, as shown in Figures 4B–4E. Strikingly, the regions of interaction between the two dimers are precisely the patches of residues predicted by the genetics to mediate cooperativity. The red patch on the gold subunit of each dimer interacts with the blue patch on the green subunit of each dimer. The individual residues predicted by the genetics to be juxtaposed at the cooperativity interface are indeed close to one another at the dimer–dimer interface in the crystal: Asp-197 and Lys-192 form an ion pair (2.9 Å) bridging the dimer–dimer interface, and the sidechains of Gln-204 and Asn-148 are 3.6 Å from one another (Figure 4D). Thus, the genetic data strongly suggest that the interactions that mediate cooperative binding of two repressor dimers to pairs of operator sites on the DNA are captured in the crystal.

Inspection of the tetramer in Figure 4B shows that only two of the four patches on the surface of the dimer are buried at the dimer–dimer interface (see also Figures 5A and 5B). The red patch on each of the green subunits and the blue patch on each of the gold subunits do not interact at the dimer–dimer interface and are exposed to solvent. While this at first seems unexpected, it can be easily reconciled with the biochemical data, since the repressor forms octamers in solution (Senear et al., 1993). Thus, the exposed patches are potential sites for further oligomerization of the CTD. This type of association arises from the unusual C2 symmetry of the tetramer. Most tetrameric proteins have D2 (three mutually perpendicular 2-fold axes) or C4 (one 4-fold axis) symmetry, in which cases the oliogomerization interface on each subunit is necessarily occluded in the tetramer, thus preventing further oligomerization. In the CTD tetramer, the 2-fold axes relating the two subunits within each dimer are not perpendicular to the 2-fold axis relating the two dimers, but rather are inclined by ~40° (Figure 4E).

The interactions at the dimer–dimer interface bury 855 $Å^2$ of solvent-accessible surface area per dimer and occur at two separate regions. The primary region of interaction involves the residues identified in the genetic studies that form the cooperativity patches. Here, the β4-β5 hairpin of the yellow subunit inserts into a pocket formed by β strand 4, and loops 1, 3, and 5 of the green subunit. The atomic interactions at this region of the dimer–dimer interface involve a small network of ion pairs (Asp-197-Lys-192 and Arg-196-Glu-188) and hydrogen bonds (Figure 4D). A secondary region of interaction between the two dimers occurs where loop 1 and loop 5 of the two yellow subunits come into contact about the 2-fold axis of symmetry (Figure 4C). Here, Ser-156 is closely hydrogen bonded to its symmetry mate (2.6 Å), and Pro-153, Pro-208, and Thr-154 participate in van der Waals interactions. Throughout the dimer–dimer interface, several ordered water molecules mediate indirect hydrogen bonds between the two CTD dimers.

It is intriguing to note that Lys-192 and Ser-149, the residues that form the active site for the RecA-mediated cleavage, also participate in interactions at the cooperativity interface (Figure 4D). Interestingly, the genetic screens designed to isolate mutants deficient in RecA-mediated cleavage (*ind*⁻ mutants) did not uncover mutations affecting Lys-192 or Ser-149. The screens employed for identifying *ind*⁻ phage demanded that the mutant phage be capable of forming stable lysogens (for example, see Gimble and Sauer, 1985). The absence of *ind*⁻ mutations affecting Lys-192 and Ser-149 is consistent with the observation that amino acid substitutions at these two residue positions disrupt cooperativity, which is essential for the maintenance of lysogeny.

A closer analysis of the structure and genetics of the dimer–dimer interface allows an assessment of the interactions that contribute significantly to the free energy of association. For example, the genetics predict that the ion pair between Asp-197 and Lys-192 is important, because replacing either of these residues with alanine abolishes cooperativity (Whipple et al., 1998). In the same region of the structure, Ser-149 is hydrogen bonded to Asp-197 (Figure 4D). Although the amino acid substitution S149F severely weakens cooperativity, the Ser-149-Asp-197 interaction does not contribute significantly to the stability of the complex because replacement of Ser-149 with alanine does not disrupt cooperativity (Whipple et al., 1998). Similarly, the interaction between Gln-204 and Asn-148 (3.6 Å) must not contribute significantly to the association because replacement of either of these residues with alanine does not detectably affect cooperativity (Whipple et al., 1998). The contribution of the salt bridge between Arg-196 and Glu-188 (Figure 4D) to the stability of the complex remains uncertain, as mutagenesis studies have not fully characterized the roles of these residues.

In summary, mapping the genetic data onto the structure of the CTD dimer strongly suggests that the interactions that mediate cooperativity have been captured in the crystal. Not only do the general regions of the repressor CTD implicated in cooperativity contact one another at the dimer–dimer interface, but also pairs of residues predicted by the genetic studies to be juxtaposed at the dimer-dimer interface are indeed found to interact in the crystal. Although the dimer–dimer interaction is not observed in solution at physiological concentrations, the C-terminal domains interact specifically and favorably when brought together by suitably positioned operator sites on the DNA or in the concentrated environment of a crystal.

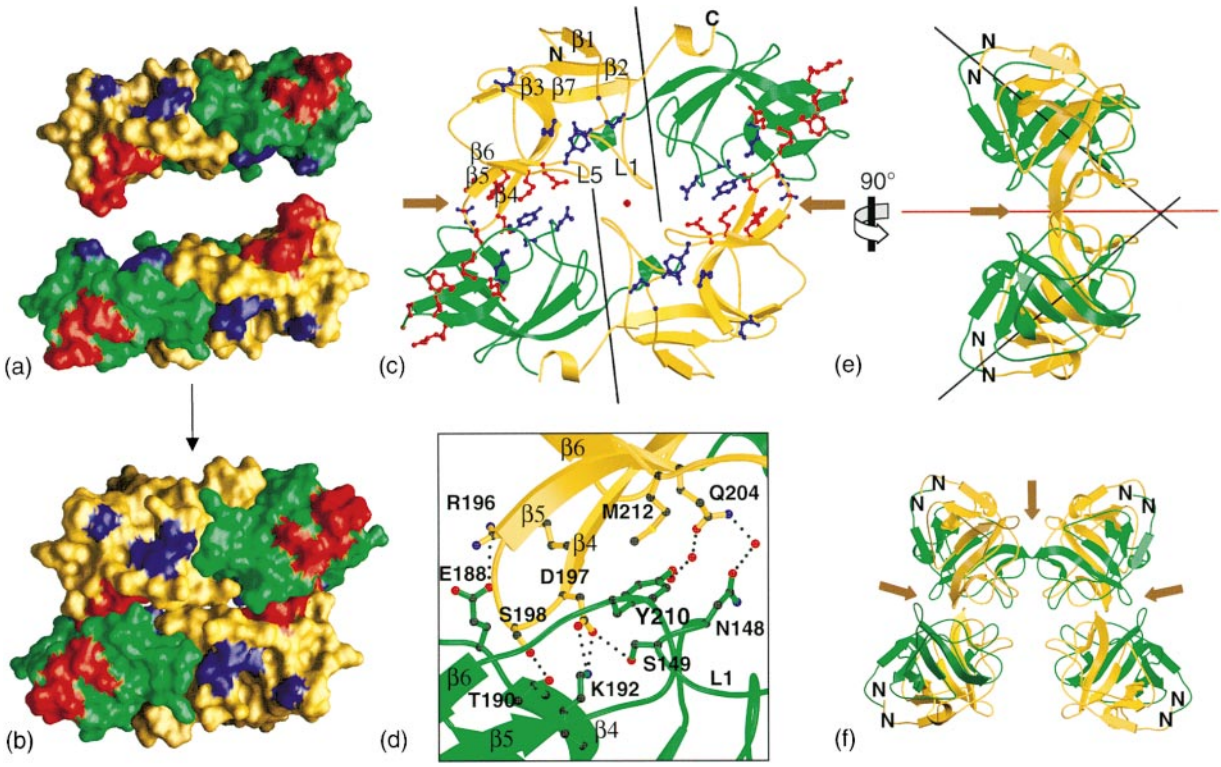

Figure 4. The Dimer–Dimer Association of the λ Repressor CTD that Mediates Cooperative Binding to DNA Is Captured in the Crystal

(A) The structure of the λ repressor CTD dimer is shown in surface representation with one subunit colored gold and the other subunit colored green. Two dimers are shown as they would approach one another to form a complex. The view of the top dimer is roughly from the bottom of Figure 1, and the bottom dimer is related to the top dimer by 180° rotation about an axis perpendicular to the plane of the figure. Residues that are affected by cooperativity mutations cluster into two patches, colored red and blue, on the surface of each monomer (the blue patch is actually comprised of two neighboring but noncontiguous regions). Within the red patch are Arg-196, Asp-197, Ser-198, Gly-199, Phe-202, Gln-204, and Met-212. Within the blue patch are Gly-147, Asn-148, Ser-149, Glu-188, Lys-192, and Tyr-210.

(B) Two dimers of the λ repressor CTD associate about a 2-fold crystallographic axis of symmetry. The interactions between the two dimers involve the patches of residues (colored red or blue) that are affected by cooperativity mutations. Specifically, the red patches on the gold subunits dock to the blue patches on the green subunits. Notice that half of the patches (the red patch on each green subunit and the blue patch on each yellow subunit) are exposed to solvent, offering potential sites for further association.

(C) Ribbon representation of the λ repressor CTD tetramer, looking down the crystallographic 2-fold axis of symmetry (same view as [B]). The crystallographic 2-fold axis, shown as a red dot in the center, relates the top dimer to the bottom dimer. The black lines indicate the 2-fold axes (noncrystallographic) that relate the two subunits within each dimer. Residues that are affected by cooperativity mutations are shown in ball-and-stick representation and are colored red or blue as indicated in (A). Notice that the interactions between the two dimers (indicated by the brown arrows) involve the red cluster of residues on each gold subunit and the blue cluster of residues on each green subunit. Also notice that the β4-β5 hairpin of the gold subunit inserts into a pocket on the green subunit.

(D) Close-up view of the atomic interactions at the dimer–dimer interface. The orientation is the same as in (B) and (C). Ion-pair and hydrogen bonding interactions bridging the dimer–dimer interface (within 3.5 Å) are shown as dotted lines. Notice that the interactions center on the ion pair between Asp-197 and Lys-192.

(E) View of the CTD tetramer looking from the left side of (C). The rotation axis shows the relation of (E) to (C). Notice that the N terminus of each subunit extends to the left side of the tetramer, with the N termini of the "top" dimer pointing up and the N termini of the "bottom" dimer pointing down. This suggests the likely orientation of the CTD tetramer with respect to the DNA, as each of the four N-terminal DNA binding domains would point to the left side.

(F) The dimer–dimer association of the λ repressor C-terminal domain can be repeated to form an octamer. The brown arrows indicate each dimer–dimer interface. Although the outer dimers (bottom left and bottom right) expose potential sites for further association, adding a fifth dimer would result in steric clashes. Notice that the N terminus of each subunit extends to the outside of the octamer, so that the N-terminal DNA binding domains of the intact repressor could fan out without steric hindrance.

Discussion

Dimerization and cooperativity are common themes in the regulation of transcription by proteins. Whereas many dimeric DNA binding proteins have been characterized structurally, it has been considerably more difficult to perform structural studies on the typically weaker interactions between proteins that mediate their cooperative binding to DNA. Cooperative binding can involve homotypic interactions, as in the case of the λ repressor, or heterotypic interactions. In eukaryotes, especially, gene activation often involves the cooperative assembly of large protein complexes on the DNA, which are stabilized by multiple weak protein-protein interactions. Cooperativity can generate sensitive biological switches by providing a steep dose-response curve, and heterotypic cooperativity can serve as a mechanism for integrating multiple regulatory inputs. However, despite the impor-

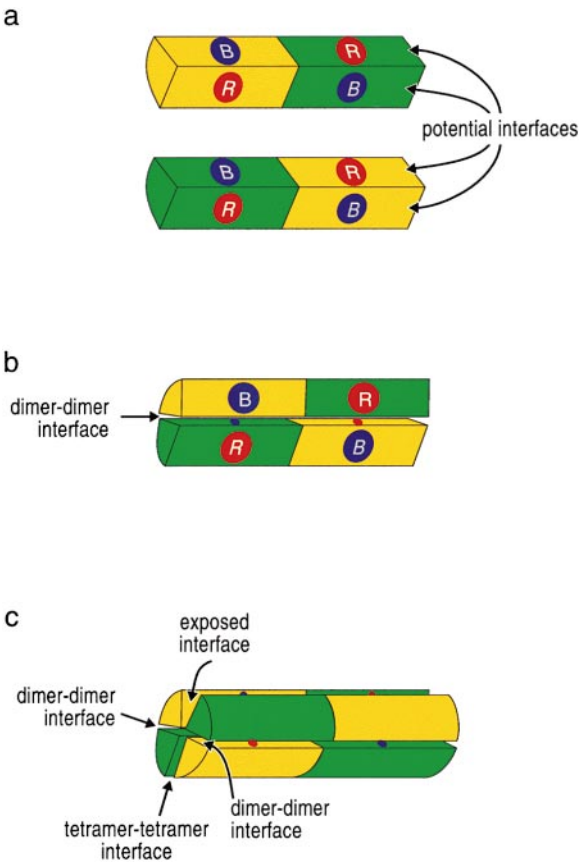

Figure 5. Model Depicting Tetramer Formation and Octamer Formation

(A) A pair of CTD dimers is shown in cartoon representation. The view is the same as in Figure 4A. Each dimer is depicted as a wedge with one subunit colored gold and the other subunit colored green. The red and blue cooperativity patches are shown schematically on the surface of each subunit.

(B) The dimers depicted in (A) have been rotated toward one another and paired to form the tetramer. The view is the same as in Figure 4B. Note that this pairing involves the lower face of the upper wedge in (A) and the upper face of the lower wedge, such that the red patches on the gold subunits dock against the blue patches on the green subunits.

(C) Two tetramers have been brought together to form an octamer. This pairing can be visualized by duplicating the tetramer shown in (B) and rotating the second copy by 180° around its long axis. The second copy can then be paired with the first such that the red and blue patches shown on the lower dimer in (B) can dock with complementary blue and red patches contributed by one of the dimers of the second tetramer (labeled tetramer–tetramer interface). Note the presence of an "exposed" interface at the top of the cylinder where the faces of the upper two dimers are neither sufficiently close to one another to pair nor sufficiently far apart to permit another dimer to enter the complex (see also Figure 4F).

tance of cooperativity for gene regulation, relatively little is known in structural detail about the underlying protein-protein interactions.

One challenge of x-ray crystallographic studies is in determining whether or not an association observed in a crystal is biologically relevant. For example, to distinguish a dimer interface from the crystal lattice contacts can be nontrivial. In the case of the UmuD′ protein, the choice of a molecular dimer (i.e., that present in solution) from the crystal lattice (Peat et al., 1996a) proved to be inconsistent with subsequent solution NMR studies (Ferentz et al., 1997). In the case of the λ repressor CTD, the wealth of genetic data available not only facilitates the assignment of the molecular dimer but also demonstrate that a dimer–dimer association observed in the crystal is relevant to the dimer–dimer interaction that results in cooperative binding to pairs of operator sites.

The two types of associations of the λ repressor CTD (the association of two monomers to form the dimer and the association of two dimers to form the tetramer) are distinguished by their strengths and their biological functions. Like many DNA binding proteins, the λ repressor must first dimerize to bind its specific recognition site on the DNA, and the stability of the repressor dimer depends primarily on the interaction of the CTDs. By contrast, the dimer–dimer association is too weak to occur off of the DNA at ordinary physiological concentrations of the repressor. The function of this higher-order interaction, which occurs when two repressor dimers are brought close to one another by the DNA, is to stabilize the repressor-operator complexes and to promote the occupancy of specific low-affinity operator sites on the phage chromosome.

The dimer interface of the CTD is consistent with interfaces seen in other oligomeric proteins (Jones and Thornton, 1996). The two monomers form an isologous, 2-fold symmetric dimer, in which an identical surface of each subunit is buried at the interface. In such an arrangement, further oligomerization (using the same interface) is not possible. The dimer interface of the CTD has few gaps or buried water molecules; the two surfaces are highly complementary.

In contrast, the dimer–dimer association of the λ repressor CTD is atypical. Although the dimer–dimer association is 2-fold symmetric, the subunits form a heterologous association: the surface of each subunit buried at the interface is not the same. Consequently, further oligomerization is possible using the same set of interactions. The interactions are almost exclusively comprised of ion pairs and hydrogen bonds and involve few apolar residues. Moreover, the dimer–dimer association involves two surfaces that are overall not highly complementary to one another. While at particular regions the interactions are intimate, throughout much of the interface there are gaps, and several of the hydrogen bonds are formed indirectly through ordered water molecules. The predominance of electrostatic interactions, modest amount of surface area buried, and limited extent of complementarity at the dimer-dimer interface are consistent with a relatively weak association that occurs only when the two dimers are brought together by the DNA.

The interaction of the two CTD dimers in the crystal is in close agreement with the genetic data, but is the architecture of the tetramer stereochemically consistent with the cooperative binding of two dimers of the intact λ repressor? The N terminus of each of the four subunits points to one side of the tetramer (the left side as viewed in Figure 4E), immediately suggesting the probable orientation of the CTD tetramer relative to the DNA. Moreover, the N termini of the "top" dimer point to the top of the tetramer, while the N termini of the "bottom" dimer point to the bottom, further orienting the CTD tetramer

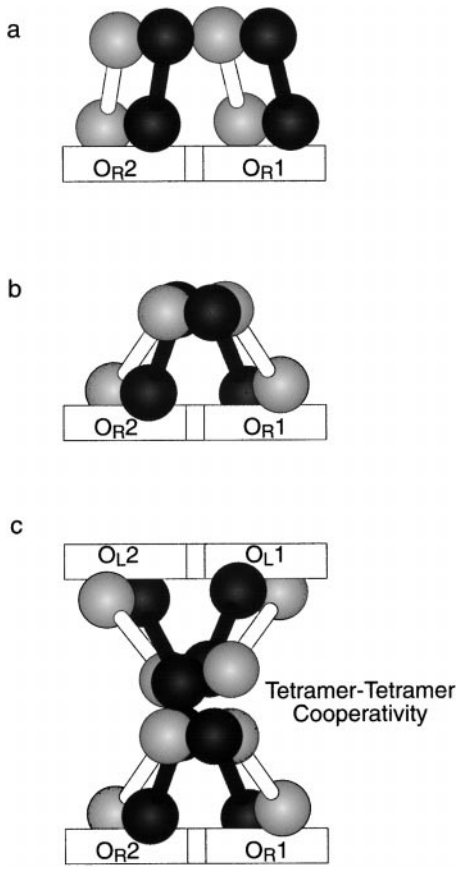

Figure 6. Models for Cooperative Binding of λ Repressor Dimers to Multiple Operator Sites

(A) A model for cooperativity is shown in which two λ repressor dimers interact using only one subunit from each dimer.

(B) A model for cooperativity is shown in which two λ repressor dimers interact using both subunits from each dimer. This type of interaction is observed in the crystal and is further supported by genetic data.

(C) A model for the cooperative binding of two λ repressor tetramers to two pairs of operators separated by several hundred base pairs. Tetramer–tetramer association has been observed to occur both in vitro and in vivo (Révet et al., 1999).

with respect to the operator sites O_R1 and O_R2. Thus, the tetramer of the CTD observed in the crystal seems to have the ideal architecture to function in the context of the intact repressor. However, a precise modeling of the overall architecture of the intact repressor complexed to the operator is not possible from the present data, as the 40-residue linker region would allow for a significant degree of flexibility between the NTD and the CTD (Weiss et al., 1983).

Although the λ repressor is predominantly dimeric at physiological concentrations ($\sim 10^{-7}$ M), at higher concentrations the repressor forms tetramers and octamers, while oligomers larger than octamers are not observed (Senear et al., 1993). It is not known if the octamer is relevant to λ physiology. However, when two pairs of operators are separated by 2000–3000 bp, two DNA-bound tetrameric complexes of the λ repressor are able to interact, resulting in the formation of a DNA loop (Révet et al., 1999). Moreover, repression of transcription in vivo from a λ P_R-lacZ fusion can be increased 4-fold by the presence of a distant pair of operator sites 3600 bp away. On the λ chromosome, the O_R and O_L regions are separated by about 2500 bp, and they are thought to regulate transcription from P_R and P_L independently. While there are no direct experimental data that suggest otherwise, the above experiment clearly demonstrates that two repressor tetramers bound to O_R and O_L could interact and that the resulting octamer could mediate repression of both P_R and P_L.

The tetramer of the CTD observed in the crystal offers a satisfying model for how the λ repressor forms an octamer. As is illustrated in Figures 4A–4C and 5A and 5B, a dimer of the CTD has two potential sites for interaction with another dimer. When two dimers associate to form a tetramer, each dimer has a second potential site for interaction that is fully exposed to solvent. Using the same interface that brings two dimers together, two tetramers of the λ repressor CTD can be brought together to form an octamer (Figures 4F and 5C). An important feature of this model for the octamer is that the N terminus of each subunit points to the outside. As a result, the N-terminal domains of the intact repressor could fan out from the CTD octamer without steric hindrance. The model clearly illustrates that oligomerization could not proceed further than the octamer. Binding a fifth dimer to this oligomer (to make a decamer) would result in steric clashes. In this way, the crystal structure provides a rational explanation for why the oligomeric state of the repressor at high concentrations is an octamer and provides a structural model for understanding how two λ repressor tetramers can interact to mediate repression and form DNA loops.

Conclusions

The structure of the λ repressor CTD in the crystalline state provides a wealth of information concerning the molecular basis of cooperativity and is remarkably consistent with previous biochemical and genetic data. The CTD mediates protein–protein interactions that result in cooperative binding of two repressor dimers to appropriately spaced operator sites on the DNA. Figure 6 illustrates two possible models for how such interactions can occur. In the first model (Figure 6A), only one subunit of each dimer contributes to the dimer–dimer interactions. In the second model (Figure 6B), both subunits of each repressor dimer contribute to the cooperative association. The crystal structure of the λ repressor CTD, in concert with genetic and biochemical data, supports the second model, and shows that further oligomerization is possible using the same interaction surfaces (Figures 4 and 5). Whether relevant to the physiology of phage λ or not, the repressor has evolved to allow the cooperative association of up to four dimers, and the crystal structure provides a model for the octamer (Figures 5C, 6C, and 4F). While a dimer–dimer association involving all four subunits may be a more general mechanism among dimeric repressors that bind to DNA cooperatively, the precise organization and number of dimers that could associate could vary in other systems. The structure of the λ repressor CTD provides a detailed model for understanding the nature of the relatively weak protein–protein interactions that mediate cooperative binding to DNA.

Table 1. Crystallographic Data, MAD Phasing, and Refinement Statistics

(A) Crystal Data

Space Group	$C222_1$
a	46.0
b	101.3
c	114.3

	hgac λ1	hgac λ2	hgac λ3	native
Resolution (Å)	20.0–2.3	20.0–2.3	20.0–2.3	17.0–1.8
Number observed	86170	66967	67688	71961
Number unique	22151	21652	21746	22468
Completeness (%)	100.0 (99.9)[a]	97.7 (98.4)	98.1 (98.6)	89.1 (58.1)
Redundancy	3.9	3.1	3.1	3.2
R_{merge}[b]	5.3 (17.6)	5.3 (20.5)	5.2 (20.1)	5.7 (10.5)
I/σ	20.5 (8.1)	16.7 (6.2)	16.6 (6.1)	10.7 (4.7)

(B) MAD Phasing

Resolution (Å)	20.0–2.5
Figure of Merit	0.64 (0.59)

Anomalous (diagonal) and dispersive (off diagonal) differences:

	λ1	λ2	λ3
λ1 (1.0070Å, peak)	0.059	0.033	0.033
λ2 (1.0090Å, edge)		0.044	0.024
λ3 (0.9829Å, remote)			0.054

(C) Refinement Statistics

Resolution (Å)	15.0–1.9
Number of reflections (working/free set)	17884/1974
Completeness (%)	92.6%
RMS deviation from ideality:	
bonds	0.006
angles	1.4
R-factor/Free R-factor (%)[c]	22.8/25.7

[a] Numbers in parentheses refer to the highest resolution shell only.
[b] $R_{merge} = \Sigma|I_h - <I>_h|/\Sigma I_h$, where $<I>_h$ is average intensity over symmetry equivalents.
[c] R-factor $= \Sigma|F_{obs} - F_{calc}|/\Sigma F_{obs}$.

Experimental Procedures

Protein Expression, Purification, and Crystallization

Residues 132–236 of the λ repressor were expressed in *E. coli* under the control of a T7 promoter using the pET-14b vector (Novagen). The CTD was expressed as an N-terminal 6-His tagged protein with an intervening thrombin proteolytic site. The protein was purified by Ni-NTA affinity chromatography (Qiagen), and the 6-His tag was removed by thrombin proteolysis (Pharmacia Biotech). A second Ni-NTA step separated the cleaved CTD from various remaining impurities. The purified CTD was dialyzed into 150 mM NaCl, 20 mM Tris, and 3 mM DTT (pH 7.4), and concentrated to 20 mg/ml. Crystals grew in 2 weeks from solutions of 1.2 M NaH_2PO_4, 1.05 M KH_2PO_4, 0.075 M hepes (pH 8.0), and 25% glycerol, and have two monomers of the CTD per asymmetric unit and a solvent content of 57%.

X-Ray Data Collection and Structure Determination

Native data were collected to 1.8 Å at 100 Kelvin at the National Synchrotron Light Source (NSLS) beamline X25 using a Brandeis B4 CCD detector (Table 1). Attempts to solve the structure by molecular replacement with the UmuD′ structure (PDB accession code 1UMU) as a search model were unsuccessful using either AmoRe (Navaza, 1994) or a genetic algorithm search procedure (Chang and Lewis, 1997). A heavy atom derivative was prepared by soaking a crystal in mother liquor with the addition of 2 mM mercuric acetate (HgAc) for 18 hr. MAD data to 2.3 Å were collected at three wavelengths on a single HgAc derivative crystal at the NSLS beamline X12B at 100 Kelvin using an ADSC Quantum-4 CCD detector. X-ray data were integrated and scaled using DENZO/SCALEPACK (Otwinowski and Minor, 1997). Two heavy atom sites were located from an anomalous difference Patterson map using a genetic algorithm search procedure (Chang and Lewis, 1994). Heavy atom sites were refined and MAD phases were calculated at 2.5 Å using SOLVE (Terwiliger and Berendzen, 1999). The MAD phases were improved by solvent flattening and histogram matching using DPHASE (G. Van Duyne, personal communication). The resulting 2.5 Å electron density map enabled the tracing of both subunits of the CTD using O (Jones et al., 1991). Although there is a 2-fold noncrystallographic symmetry (NCS) axis, the electron density map used to fit the structure was not averaged. The electron density for the N-terminal residues Thr-132-Lys-135 was absent for both subunits, and these residues were not included in the model.

The structure was refined using Crystallography and NMR System (Brünger et al., 1998). Refinement included simulated annealing (Adams et al., 1997), restrained isotropic temperature factor refinement, a bulk solvent correction, and an overall anisotropic temperature factor correction. Throughout the refinement, 10% of the data (1974 reflections) were omitted for calculation of the free R-factor (Brünger, 1992). Two-fold NCS restraints were imposed on all atoms of the protein during the early rounds of refinement but were completely released during later stages. Both the R-factor and free R-factor remained above 30% until the NCS-restraints were released entirely. Solvent-accessible surface area calculations used the algorithm of Lee and Richards (1971) with a probe radius of 1.4 Å. Figures were prepared using MOLSCRIPT (Kraulis, 1991), RASTER3D (Merritt and Bacon, 1997), GRASP (Nicholls et al., 1991), and O (Jones et al., 1991).

Acknowledgments

We thank Drs. Hillary C. M. Nelson and Simon Dove for critical reading of the manuscript, Dr. M. Capel at the National Synchrotron Light Source beamline X12B for useful discussions, Dr. Carlo Petosa

for construction of the λ repressor CTD expression vector, and Renate Hellmis for expert artwork. The work was supported by National Institutes of Health (NIH) grants to M. L. and A. H. and a NIH National Research Service Award to C. E. B. and is based on research conducted at the NSLS beamlines X25 and X12B at Brookhaven National Laboratory.

Received March 14, 2000; revised May 8, 2000.

References

Ackers, G.K., Johnson, A.D., and Shea, M.A. (1982). Quantitative model for gene regulation by λ phage repressor. Proc. Natl. Acad. Sci. USA *79*, 1129–1133.

Adams, P.D., Pannu, N.S., Read, R.J., and Brünger, A.T. (1997). Cross-validated maximum likelihood enhances crystallographic simulated annealing refinement. Proc. Natl. Acad. Sci. USA *94*, 5018–5023.

Beamer, L.J., and Pabo, C.O. (1992). Refined 1.8 Å crystal structure of the λ repressor-operator complex. J. Mol. Biol. *227*, 177–196.

Beckett, D., Burz, D.S., Ackers, G.K., and Sauer, R.T. (1993). Isolation of lambda repressor mutants with defects in cooperative operator binding. Biochemistry *32*, 9073–9079.

Benson, N., Adams, C., and Youderian, P. (1994). Genetic selection for mutations that impair the co-operative binding of lambda repressor. Mol. Microbiol. *11*, 567–579.

Brünger, A.T. (1992). Free R value: a novel statistical quantity for assessing the accuracy of crystal structures. Nature *355*, 472–475.

Brünger, A.T., Adams, P.D., Clore, G.M., DeLano, W.L., Gros, P., Grosse-Kunstleve, R.W., Jiang, J.S., Kuszewski, J., Nilges, M., Pannu, N.S., et al. (1998). Crystallography and NMR system: a new software suite for macromolecular structure determination. Acta Crystallogr. D *54*, 905–921.

Burz, D.S., and Ackers, G.K. (1994). Single-site mutations in the C-terminal domain of bacteriophage λ cI repressor alter cooperative interactions between dimers adjacently bound to O_R. Biochemistry *33*, 8406–8416.

Burz, D.S., Beckett, D., Benson, N., and Ackers, G.K. (1994). Self-assembly of bacteriophage λ cI repressor: effects of single-site mutations on the monomer-dimer equilibrium. Biochemistry *33*, 8399–8405.

Bushman, F.D., Shang, C., and Ptashne, M. (1989). A single glutamic acid residue plays a key role in the transcriptional activation function of lambda repressor. Cell *58*, 1163–1171.

Chang, G., and Lewis, M. (1997). Molecular replacement using genetic algorithms. Acta Crystallogr. D *53*, 279–289.

Chang, G., and Lewis, M. (1994). Using genetic algorithms for solving heavy-atom sites. Acta Crystallogr. D *50*, 667–674.

Cohen, S., Knoll, B., Little, J.W., and Mount, D.W. (1981). Preferential cleavage of phage λ repressor monomers by recA protease. Nature *284*, 182–184.

Dodson, G., and Wlodawer, A. (1998). Catalytic triads and their relatives. Trends. Biochem. Sci. *23*, 347–352.

Ferentz, A.E., Opperman, T., Walker, G.C., and Wagner, G. (1997). Dimerization of the UmuD′ protein in solution and its implications for regulation of SOS mutagenesis. Nat. Struct. Biol. *4*, 979–983.

Gimble, F.S., and Sauer, R.T. (1985). Mutations in bacteriophage lambda repressor that prevent RecA-mediated cleavage. J. Bacteriol. *162*, 147–154.

Gimble, F.S., and Sauer, R.T. (1986). λ repressor inactivation: properties of purified *ind*⁻ proteins in the autodigestion and RecA-mediated cleavage reactions. J. Mol. Biol. *192*, 39–47.

Gimble, F.S., and Sauer, R.T. (1989). λ repressor mutants that are better substrates for RecA-mediated cleavage. J. Mol. Biol. *206*, 29–39.

Griffith, J., Hochschild, A., and Ptashne, M. (1986). DNA loops induced by cooperative binding of lambda repressor. Nature *322*, 750–752.

Guarente, L., Nye, J.S., Hochschild, A., and Ptashne, M. (1982). Mutant lambda phage repressor with a specific defect in its positive control function. Proc. Natl. Acad. Sci. USA *79*, 2236–2239.

Hochschild, A., and Ptashne, M. (1986). Cooperative binding of λ repressors to sites separated by integral turns of the DNA helix. Cell *44*, 681–687.

Hochschild, A., Irwin, N., and Ptashne, M. (1983). Repressor structure and the mechanism of positive control. Cell *32*, 319–325.

Johnson, A.D., Meyer, B.J., and Ptashne, M. (1979). Interactions between DNA-bound repressors govern regulation by the λ phage repressor. Proc. Natl. Acad. Sci. USA *76*, 5061–5065.

Jones, S., and Thornton, J.M. (1996). Principles of protein-protein interactions. Proc. Natl. Acad. Sci. USA *93*, 13–20.

Jones, T.A., Zhou, J.-Y., Cowan, S.W., and Kjeldgaard, M. (1991). Improved methods for building protein models in electron density maps and the location of errors in these models. Acta Crystallogr. A *47*, 110–119.

Jordan, S.R., and Pabo, C.O. (1988). Structure of the lambda complex at 2.5 Å resolution: details of the repressor-operator interactions. Science *242*, 893–899.

Kraulis, P. (1991). MOLSCRIPT: a program to produce both detailed and schematic plots of protein structures. J. Appl. Crystallogr. *24*, 946–950.

Kuldell, N., and Hochschild, A. (1994). Amino acid substitutions in the −35 recognition motif of σ^{70} that result in defects in phage lambda repressor-stimulated transcription. J. Bacteriol. *176*, 2991–2998.

Lee, B., and Richards, F.M. (1971). The interpretation of protein structures: estimation of static accessibility. J. Mol. Biol. *55*, 379–400.

Li, M., Moyle, H., and Susskind, M.M. (1994). Target of the transcriptional activation function of phage λ cI protein. Science *263*, 75–77.

Lin, L.L., and Little, J.W. (1989). Autodigestion and RecA-dependant cleavage of *ind*⁻ mutant LexA proteins. J. Mol. Biol. *210*, 439–452.

Little, J.W. (1984). Autodigestion of lexA and phage lambda repressors. Proc. Natl. Acad. Sci. USA *81*, 1375–1379.

Maniatis, T., and Ptashne, M. (1973). Multiple repressor binding at the operators in bacteriophage λ. Proc. Natl. Acad. Sci. USA *70*, 1531–1535.

Maniatis, T., Ptashne, M., Backman, K., Kield, D., Flashman, S., Jeffrey, A., and Maurer, R. (1975). Recognition sequences of repressor and polymerase in the operators of bacteriophage λ. Cell *5*, 109–113.

Merritt, E.A., and Bacon, D.J. (1997). Raster3D: photorealistic molecular graphics. Methods Enzymol. *277*, 505–524.

Meyer, B.J., and Ptashne, M. (1980). Gene regulation at the right operator (OR) of bacteriophage λ III. λ repressor directly activates gene transcription. J. Mol. Biol. *139*, 195–205.

Meyer, B.J., Maurer, R., and Ptashne, M. (1980). Gene regulation at the right operator (O_R) of bacteriophage λ II. O_R1, O_R2, and O_R3: their roles in mediating the effects of repressor and cro. J. Mol. Biol. *139*, 163–194.

Navaza, J. (1994). AMoRe: an automated package for molecular replacement. Acta Crystallogr. D *50*, 157–163.

Nicholls, A., Sharp, K.A., and Honig, B. (1991). Protein folding and association: insights from the interfacial and the thermodynamic properties of hydrocarbons. Prot. Struct. Funct. Genet. *11*, 281–296.

Otwinowski, Z., and Minor, W. (1997). Processing of x-ray diffraction data collected in oscillation mode. Methods Enzymol. *276*, 307–326.

Pabo, C.O., and Lewis, M. (1982). The operator-binding domain of λ repressor: structure and DNA recognition. Nature *298*, 443–447.

Pabo, C.O., Sauer, R.T., Sturtevant, J.M., and Ptashne, M. (1979). The λ repressor contains two domains. Proc. Natl. Acad. Sci. USA *76*, 1608–1612.

Peat, T.S., Frank, E.G., McDonald, J.P., Levine, A.S., Woodgate, R., and Hendrickson, W.A. (1996a). Structure of the UmuD′ protein and its regulation in response to DNA damage. Nature *380*, 727–730.

Peat, T.S., Frank, E.G., McDonald, J.P., Levine, A.S., Woodgate, R., and Hendrickson, W.A. (1996b). The UmuD′ protein filament and its

potential role in damage induced mutagenesis. Structure *4*, 1401–1412.

Ptashne, M. (1992). A Genetic Switch (Cambridge, MA: Cell Press and Blackwell Scientific Publications).

Révet, B., Wilcken-Bergmann, B.V., Bessert, J., Barker, A., and Müller-Hill, B. (1999). Four dimers of λ repressor bound to two suitably spaced pairs of λ operators form octamers and DNA loops over large distances. Curr. Biol. *9*, 151–154.

Sauer, R.T. (1979). Molecular characterization of λ repressor and its gene *c*I. Ph.D. Thesis, Harvard University, Cambridge, Massachusetts.

Sauer, R.T., Ross, M.J., and Ptashne, M. (1982). Cleavage of the λ and P22 repressors by *recA* protein. J. Biol. Chem. *257*, 4458–4462.

Senear, D.F., Laue, T.M., Ross, J.B., Waxman, E., Eaton, S., and Rusinova, E. (1993). The primary self-assembly reaction of bacteriophage lambda *c*I repressor dimers is to octomer. Biochemistry *32*, 6179–6189.

Slilaty, S.N., and Little, J.W. (1987). Lysine-156 and serine-119 are required for LexA repressor cleavage: a possible mechanism. Proc. Natl. Acad. Sci. USA *84*, 3987–3991.

Terwiliger, T.C., and Berendzen, J. (1999). Automated structure solution for MIR and MAD. Acta Crystallogr. D *55*, 849–861.

Weiss, M.A., Karplus, M., Patel, D.J., and Sauer, R.T. (1983). Solution NMR studies of intact λ repressor. J. Biomol. Struct. Dyn. *1*, 151–157.

Whipple, F.W., Hou, E.F., and Hochschild, A. (1998). Amino acid-amino acid contacts at the cooperativity interface of the bacteriophage λ and P22 repressors. Genes Dev. *12*, 2791–2802.

Whipple, F.W., Kuldell, N.H., Cheatham, L.A., and Hochschild, A. (1994). Specificity determinants for the interaction of λ repressor and P22 repressor dimers. Genes Dev. *8*, 1212–1223.

Protein Data Bank ID Codes

Coordinates have been deposited in the Protein Data Bank under ID code 1F39.